

Post-discharge kinetics associated with a plasmachemical nucleophilic substitution and application to the analysis of plasma activated CO

AVALY DOUBLA^{1,2} and JEAN-LOUIS BRISSET^{2,*}

¹Laboratoire de Chimie Minérale, Département de Chimie Inorganique, Faculté des Sciences, Université de Yaoundé I, BP 812, Yaoundé, Cameroun

²Laboratoire d'Electrochimie (L.E.I.C.A), U.F.R. des Sciences et Techniques de l'Université de Rouen, F-76821, Mont-Saint-Aignan-Cédex, France

(*author for correspondence, e-mail: Jean-Louis.Brisset@univ-rouen.fr)

Received 22 November 2004; accepted in revised form 6 July 2005

Key words: carbon monoxide, D.C. corona discharge, nucleophilic substitution reactions, pentacyano(carbonyl)ferrate [II], post-discharge reaction

Abstract

The UV-visible absorbance spectra of aqueous solutions of pentacyano (N.methyl pyrazinium) ferrate(II) complex exposed to the flux of neutral activated species of a DC corona discharge in CO at atmospheric pressure are deeply modified: the blue color of the starting complex fades, which is not observed in ordinary conditions. The overall kinetic law is found to be zero-order and interpreted in terms of ligand exchange reaction (i.e., a nucleophilic substitution reaction induced by D.C. corona discharge) by comparison with literature result relevant to the exchange of other ligands in solution. Additionally, post-discharge phenomena induced by the plasma treatment are also observed. They obey an overall 1st order kinetic law under our working conditions. The influence of the most salient working parameters on the post discharge kinetic rate is examined. The electric power provided to the discharge is probably the most important factor for controlling the post-discharge kinetic rate. The results obtained also suggest a new analytical technique to quantify activated CO.

1. Introduction

The chemical reactivity of carbon monoxide is usually limited to a few particular examples although some of them are of major importance, such as the complex formation of CO with haemoglobin or related substrates, the formation of carbonyl metals or the adsorption on particular crystal faces of metals. Additionally, the oxidation-reduction reactions occurring in smelting furnaces or the chemical characterisation of CO are important. In organic chemistry the oxo syntheses which also involve H₂ or H₂O and olefin molecules have been the subject of much work and many patents.

Another aspect of the reactivity of CO concerns coordination chemistry and the ability of the molecule to form complexes. The mechanisms of the CO substitution on carbonyl metals are now well known through the work of Basolo [1, 2]. Ligand exchange reactions in solution were investigated on a particular family of Fe(II) complexes, the pentacyano(L)ferrate(II) series (i.e., Fe(CN)₅L, also referred to as *feL*, where L is a labile ligand) [3–9]. Numerous experimental results relevant to the substitution reaction of the odd ligand

by a Lewis base (e.g., a nitrogen or sulphur containing moiety) were reported [3–10]. Special emphasis was devoted to the exchange mechanism in solution: a model concerning methylpyrazinium ferrate (II), later referred to as *fempz*, was proposed by Toma and Malin [10]. This model involving a steady state approximation for the *fe* moiety, was later developed and largely accepted [3–5].

CO is a ligand which presents unusual behaviour, by simultaneously displaying donor and acceptor character with metals. It is thus involved in conventional Lewis acid base reactions and even displays back-bonding [11] which increases the strength of the metal–carbon bond. However, our attempts to realise the direct substitution of *mpz* by CO in the *fempz* complexes by bubbling the gas at atmospheric pressure in an aqueous solution of *fempz* failed, whereas the exchange reaction of the odd ligand by some other entering group (e.g., an amine or a sulphur containing moiety) was easily performed [3–6, 10] in aqueous solution, as mentioned. The formation of *feCO* from *fe(H₂O)* was reported by Toma et al. [7] and the photochemistry of the pentacyanocarbonylferrate (II) was previously investigated by Vogler and Kunkely [9].

No attempt at ligand substitution under corona discharge has been reported, as far as we know. We resumed examining the question, assuming that the energy of the CO molecules would be increased in the corona discharge and the activated molecules would then become able to enter a substitution reaction.

We operated in a similar way as for the ligand exchange reactions previously investigated in solution to illustrate the specific reactivity of these corona activated species. We selected an aqueous solution of the blue complex pentacyano (N.methylpyrazinium)ferrate(II), later referred to as *fempz* as a suitable starting material. When the complex solution is exposed to the flux of the activated CO*, its colour fades and the solution becomes colourless, which does not occur in the absence of discharge. This feature suggests that a ligand exchange reaction may account for the observed phenomena.

Additionally, we investigated the kinetics of the reported colour change, and also found that the reaction went on *in the absence* of discharge, so that we report on the relevant post-discharge phenomena.

The plasma induced ligand exchange reactions are faster than most of the substitution kinetics performed on the same complex, *fe(mpz)*, without discharge. These preliminary results also suggest that specific chemical reactions may be performed by CO* molecules or more generally, that vibrationally or/and electronically excited molecules may enter chemical reactions that do not take place under normal conditions. Thus, we conclude that the reported reaction may be used to account for activated CO.

In this study, the active species are generated by the discharge burning in the gas phase. A matching technique referred to as Contact Glow Discharge Electrolysis (CGDE) and investigated by several authors [12–17] involved one immersed electrode and was found effective in breaking down aromatic pollutants. The use of electric discharges in aqueous solutions, and especially pulsed corona discharges with immersed electrodes, was more recently considered as an efficient technique for pollution abatement [18–21].

2. Experimental section

2.1. Experimental device

The corona discharge used was a modified D.C. point to plane device operated at atmospheric pressure of CO and at ambient temperature. The reactor (Figure 1) was a silica tube (inner diameter 2.8 cm) fitted with a silica holder of small volume ($V=3.5$ ml) to contain the aqueous solutions of starting complex. The distance between the holder and the point electrode was controlled ($5 < d$ (mm) < 10) and fixed at $d=8$ mm for most experiments.

The stainless steel electrode layout used for this study is referred to as “parallel layout” [22], i.e., the point

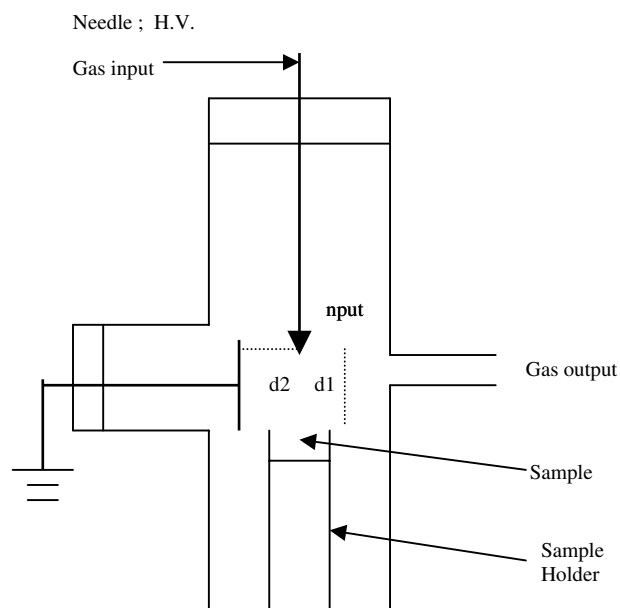


Fig. 1. Experimental set-up of the corona reactor with parallel point and plane electrodes.

electrode connected to the HV source was disposed parallel to the plane earthed electrode and perpendicular to the liquid surface (Figure 1). This layout allowed :

- (i) to differentiate the chemical reactivity of the ions from the chargeless species. The latter are carried by the electric wind, along the axis of the point electrode, while the charged species are affected by the electric field lines. The liquid target is thus exposed to the mere flux of the chargeless species, and the treatment result would not depend on the discharge polarity in our working conditions.
- (ii) to create significant electric fields, without turning to the arc, which allows the discharge to be stable and chemically efficient.
- (iii) to transfer a part of the electric energy of the discharge to the neutral species, so that they induce relevant chemical reactions and generate changes in the treated substrate.

The electric source was a HV generator delivering a stabilised DC current, with a maximum voltage fall of 30 kV. The feeding CO flux was controlled by a mass flow-meter and fixed at $6.67 \text{ cm}^3 \text{ s}^{-1}$. The plasma reactor was limited by both point and plane electrodes and the silica walls.

2.2. Working conditions

Plasma source: D.C. conditions; $10 < U$ (kV) < 30 and $20 < I$ (μA) < 100 .

Substrates: aqueous solutions of pentacyano(N.methylpyrazinium)ferrate(II) *fempz* or pentacyano(pyridine)ferrate(II), referred to as *fepy*, synthesised in the laboratory [3–5, 10].

Before any experiment the reactor was washed with acetone to get rid of the residues on the reactor walls and on the electrodes, and then dried in air. The sample

holder was filled with the solution of the starting complex feL and placed in the reactor. CO was introduced into the reactor through a hollow needle which also acted as the HV electrode. The device allowed the whole flux of CO to be excited by the discharge [22]. A flow of CO was introduced in the reactor before the discharge was switched on, so that no air remained in the reactor.

2.3. Analysis procedure

The most suitable analysis technique is UV-visible absorbance spectrophotometry of the treated solution. An aliquot of the treated solution was sampled by using a syringe and disposed in a 1-cm spectrophotometer cell fitted with a PTFE stopper to limit the contact with the atmosphere. The absorbance measurements were performed at 655 nm, i.e. at the absorption peak of the $fempz$ complex ($\epsilon_{655} = 12022 \text{ cm}^{-1} \text{ mol}^{-1} \text{ l}$), or at the absorption peaks of the pyridine ferrate, after the solution had been exposed to the plasma for various treatment times t^* .

The reaction products could not be isolated for three reasons: (i) the starting concentration of $fempz$ was very low (around 0.1 mol l^{-1}), and so that the product at the end of the reaction was expected to be equally low, (ii) spectral and electrochemical investigation provided results in agreement with the literature data for identifying the reaction product, and (iii) the pentacyano(L)ferrate complexes are known to be very sensitive to the contact with metal or rubber, which prevents the preparation of large quantities of the solid compound. Thus, no attempt to prepare the solid complex was undertaken, since it was not within the scope of the study, and no analysis of the solid product was subsequently available.

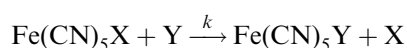
The voltammetry study of the reaction product showed no reduction signal, but only an oxidation wave (half-wave potential : 1.050 V/NHE) close to the oxidation wall of the solvent, which indicated the presence of a reducer.

3. Experimental results and discussion

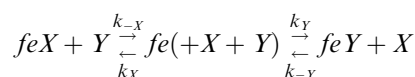
3.1. Evidence of plasma-chemical nucleophilic substitution reactions

3.1.1. Kinetic model of ligand exchange reaction in solution (in the absence of discharge)

The considered overall reaction for NS studies occurring in solution and *in the absence of discharge* is summed up as:



and corresponds to the following two-step kinetic model already considered [3–10].



A development of the model leads to

$$\frac{dx}{dt} = \frac{k_X k_{-Y} C_X + k_Y k_{-X} C_Y}{k_X C_X + k_Y C_Y} \times (x_\infty - x) = \lambda(x_\infty - x)$$

which denotes a pseudo first-order reaction in solution, when referred to the equilibrium state (x_∞) which is experimentally verified. The formal rate constant λ then depends on the ratio of the activities of entering and leaving ligand C_Y/C_X and tends to k_{-X} when the ratio is high enough.

This model is developed for ligand exchange reactions in solution and can only give direction in the present case which involves gas-liquid reactions.

3.1.2. Evidence of a plasma-chemical NS reaction

As previously mentioned, we did not observe any change in the $fempz$ solutions resulting from a mere CO bubbling in the absence of discharge.

To check that nucleophilic substitution reactions may be performed *under plasma conditions*, a dilute aqueous solution of pentacyano(mpz)ferrate(II) [$C_{fempz} = 8.31 \times 10^{-5} \text{ mol l}^{-1}$] was exposed to the positive corona discharge in CO, with the working parameters: $U = 25.5 \text{ kV}$; $I = 80 \text{ }\mu\text{A}$; $d_1 = 18 \text{ mm}$; $d_2 = 8 \text{ mm}$. The initial blue colour gradually faded, so that the concentration of the $fempz$ complex was reduced to $6.5 \times 10^{-5} \text{ mol l}^{-1}$ for a 600s treatment, while the complex $feCO$ formed accordingly. Investigating the reaction appeared to be delicate because the target solution continued to fade during the sampling and measurement times (i.e., during operations performed in the absence of the discharge).

Aliquots of the plasma treated solution were sampled for various exposure times t^* (min) and the relevant spectra recorded. The reaction product spectrum [absorbance peaks at 300 nm; 230 nm and 210 nm, with $\epsilon_{230} \approx 8000 \text{ cm}^{-1} \text{ mol}^{-1} \text{ l}$], agreed with the literature data [8]; and did not depend on the leaving ligand (i.e., mpz or substituted pyridine). Additionally, it completely differed from those of the aquo-ferrates $fe^{II}(\text{H}_2\text{O})$ [$\lambda = 455 \text{ nm}$] and $fe^{III}(\text{H}_2\text{O})$ [$\lambda = 394 \text{ nm}$], so that neither the mere exchange of mpz by water could hold nor any oxidation phenomena could be supported.

No special odour could be detected when the discharge was burning.

The voltammetry signal indicated that a reducer was present in the solution and that its oxidation took place at 1.05 V/NHE , in agreement [8] with literature data ($E^\circ = 1.18 \text{ V/NHE}$ in slightly different conditions).

Several arguments back up the assumption of the formation of the carbonyl complex:

- the reaction was observed in solution, as were the other reported examples of ligand exchange reactions involving pentacyanoferrates or, more precisely, it took place *at the liquid plasma interface*.

- the spectrum of the reaction product did not depend on the leaving ligand which would seem to indicate that CO, H₂O (or derivatives) was involved as the odd ligand.
- the known absorbance spectra of the aquo complexes $fe^{II}H_2O$ and $fe^{III}H_2O$ complexes differed from that of the reaction product, which eliminated the aquo complexes as the final product.
- the spectrum of the reaction product presented the same absorption bands as those reported in the literature [8] for Fe^{II}(CN)₅CO.
- the lack of specific odour over the solution prevented from the formation of ozone (which is known not to be favoured by the presence of water) or carbon suboxide C₃O₂.
- the voltammetric study of the product showed that no oxidised species was present in solution and agreed [8] with the formation of the reduced complex Fe^{II}(CN)₅CO. The matching formation of the yellow oxidised complex Fe^{III}(CN)₅CO can all the more be disregarded that the relevant electronic spectrum [8] presented a charge transfer band at 452 nm.

The assumption of the corona induced formation of the carbonyl complex $fe^{II}CO$ from $fempz$ may then be considered as verified, since the compound resulting from the electric discharge treatment presented spectral and electrochemical characteristics in close agreement with the pertinent literature.

Further investigation on the product was not found necessary to fulfil the purpose of this work.

3.2. Kinetic aspect of the plasmachemical reaction

3.2.1. General considerations

Several experiments performed under the same general conditions confirm that the starting solute is strongly affected by the species formed in the discharge.

It can be reasonably assumed that the reaction actually takes place at the liquid gas interface. We also guess that it implies discharge activated species, since the reaction was not observed in the absence of discharge. The nature of the active species was not investigated, because we focused on the chemical reaction and preferred to let spectroscopy specialists deal with the question to bring more precise information on the involved species. However, the species ($a^3\Pi$) CO or ($^4\Sigma$) CO, the energy of which is around 6 eV above the ground state, i.e., in the energy range usually obtained in corona discharge, might be good candidates.

Other species (e.g., OH, O₂, O, O₃, H₂O₂ and various carbon oxides CO₂, C₃O₂,...) could potentially form in the discharge. Most of these species must be discarded, due to their strong oxidising character which is largely involved in plasma pollution abatement or/and plasma bio-decontamination (e.g., E° OH/H₂O = 2.85 V/NHE; E° O/H₂O = 2.42 V/NHE; E° O₃/H₂O = 2.07 V/NHE; E° H₂O₂/H₂O = 1.68 V/NHE). If these species did form, they would readily react with CO and with the reduced

starting ferrate and yield CO₂ and oxidised complex, a result which has not been experimentally observed.

The evil smelling C₃O₂ was not detected, presumably because it reacts vigorously with water to yield the malonic acid, and might thus be responsible for the acid effect observed on pure water. However the effect is limited for the ferrate solutions, since the leaving ligand acts as a base and yields a pH-buffered medium.

All the experiments show that the solute goes on fading as the solution is sampled and the absorbance measured (Figure 2), so that it is quite impossible to get significant absorption measurements providing reliable information about the kinetic law. However a mere qualitative approach to the interface phenomena may be proposed as follows. The $fempz$ complex has a matching hydrophobic/hydrophilic character, respectively through the mpz ligand and the CN groups, which leads the complex to position at the liquid /gas interface with the mpz group preferably exposed to the discharge and to favour the attack of the impinging reactive CO. The formation of $feCO$ will then be governed by the flux of reactive CO, or better by the slow diffusion of $fempz$ to the surface.

This view is consistent with an apparent 1st order reaction.

3.2.2. Polarity of the discharge

The nucleophilic substitution reaction under corona discharge conditions was studied for the positive and negative polarities to show the general character of the feature, and under various values of the working parameters to illustrate their influence on the kinetic rate.

Similar results were observed for the ligand exchange in positive and negative discharge. However the concentration in the reaction products was higher for a positive corona than for a negative one for the same

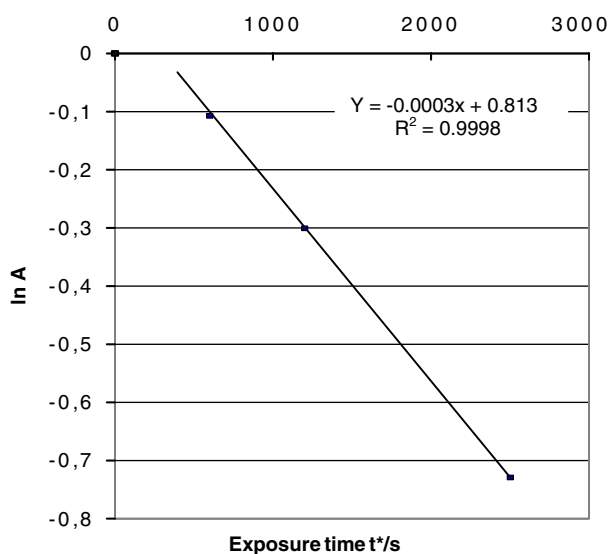


Fig. 2. Decrease in the absorbance A_{655} of the plasma treated $fempz$ solution with the treatment time t^* : plot $\ln A$ vs t^* (negative discharge ; $I = 50 \mu A$; $Q_{co} = 6.67 \text{ cm}^3 \text{ s}^{-1}$; $d_1 = 18 \text{ mm}$; $d_2 = 8 \text{ mm}$).

treatment time t^* , which is the sign of a slower mechanism in negative discharge. This suggests a different mechanism or, more likely, that the flux of activated CO^* provided by a negative discharge is less important than that provided by a positive corona. This feature confirms that the neutral species flux of a positive corona is chemically more efficient than the negative discharge one, as already pointed out for acid–base properties in humid air [23]. The following reported data are relevant to positive discharges.

For a negative corona, the concentration of the reaction products increases with the intensity of the current and with the electrode gap, that is with factors which govern the flux of activated CO (i.e., the concentration in CO^* and the residence time of the relevant species in the reactor). The same kinetic effects result from the increase in the treatment time for both discharge polarities.

This feature favours the general character of the study. We have now to detail how the discharge parameters (i.e., the treatment time t^* or the current intensity of the discharge) govern the kinetic parameters of the post-discharge reaction.

3.3. Post-discharge kinetics

The blue *fempz* solution rapidly fades when it is exposed to the flux of the carbon monoxide activated in a corona discharge for the treatment time t^* , so that the concentration of the *fempz* complex decreases and *feCO* forms. The *ex-situ* spectral analysis of the target solution exposed to the plasma for a time t^* and the absorbance

measurements at the time t after sampling show two important post-discharge phenomena:

The plasma treated solution continues to fade when the discharge is switched off or when the sampled solution is brought out of the reactor in a closed spectrometer cell: the absorbance decreases as the post-discharge time t increases. This means that (i) the substitution reaction goes on in the absence of discharge, i.e., when activated CO^* is no longer being formed, and long after the activated CO^* time life, (ii) the reaction involves the CO present at the liquid surface or dissolved in the liquid phase, although its solubility in water is limited (around 0.9 mmol l^{-1} at $25 \text{ }^\circ\text{C}$). If so, the exchange reaction should have been observed in the absence of discharge by bubbling CO. The solubility of CO is about 9 times the *fempz* concentration considered in this study, so that the limiting species cannot be CO but more likely *fempz* and (iii) the rate of the post-discharge substitution reaction is given from absorbance measurements, and affected by the treatment time t^* and the current intensity I of the discharge.

For example, the log plots $\ln|A_\infty - A_t| = f(t)$ relevant to the absorbance of a target solution exposed to the plasma for $t^* = 10 \text{ min}$ (or $t^* = 15 \text{ min}$) linearly decrease in post-discharge conditions (Figure 3), which denotes a 1st order mechanism. The relevant slopes k_{10} and k_{15} of the lines for $t^* = 10 \text{ min}$ or $t^* = 15 \text{ min}$ indicate the post-discharge reaction rates and increase with the treatment time t^* : $k_{10} = 7.11 \times 10^{-4} \text{ s}^{-1}$ and $k_{15} = 9.83 \times 10^{-4} \text{ s}^{-1}$ respectively. Also, the k values and the origin line up in a plot k vs t^* ($k = 10^{-6} t^* + 10^{-5}$; $R^2 = 0.996$) as illustrated in Figure 4.

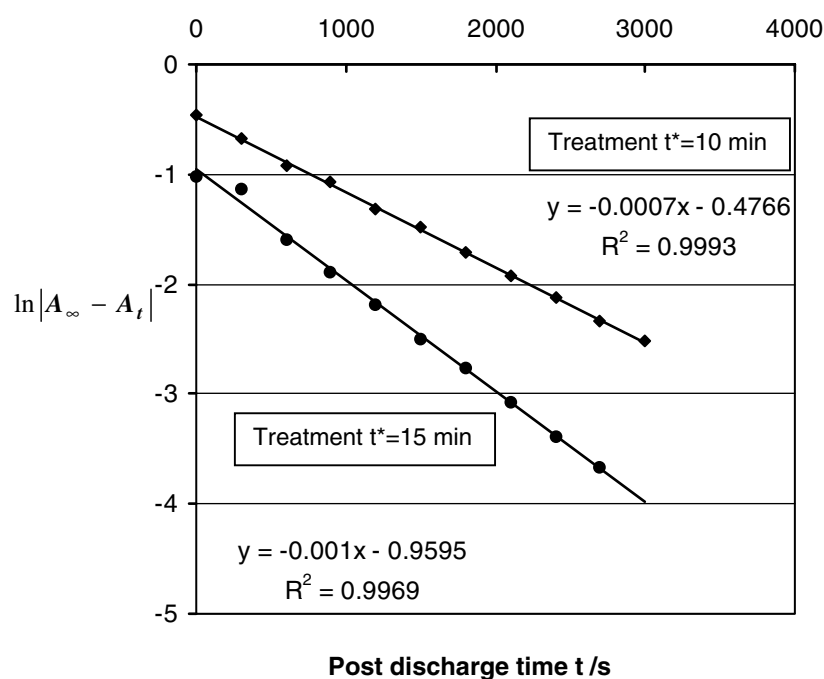


Fig. 3. Time dependant decrease in the absorbance ($\ln A_{655}$) of the pentacyano(N.methyl-pyrazinium)ferrate(II) solution in post-discharge conditions as a function of the post-discharge time t (s) for two treatment times t^* (i.e., 10 and 15 min; relevant post-discharge constants $k_{10} = 7.11 \times 10^{-4} \text{ s}^{-1}$; $k_{15} = 9.83 \times 10^{-4} \text{ s}^{-1}$). Corona discharge conditions: $U = 18 \text{ kV}$; $d_1 = 16 \text{ mm}$; $d_2 = 6 \text{ mm}$; $Q_{\text{co}} = 6.67 \text{ cm}^3 \text{ s}^{-1}$; $I = 14 \text{ } \mu\text{A}$.

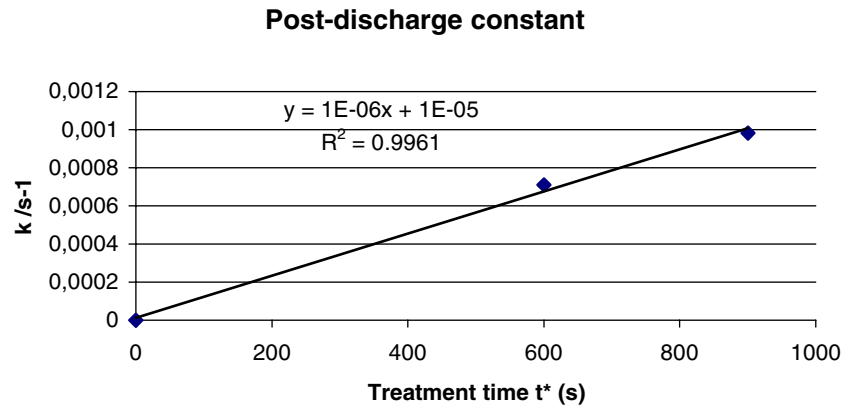


Fig. 4. Variation of the post-discharge kinetic constant k with the treatment time t^* (same data as in Figure 3).

3.3.1. Kinetic lag

In addition, the line $\ln |\Delta A_{655}| = f(t^*)$ does not intercept the axis $t^* = 0$ at the absorbance value measured for $t^* = 0$: one can estimate (Figure 2) around 3 min the time elapsed before the reaction starts. This time may be correlated to that needed to saturate with the gas the aqueous thin layer in contact with the plasma.

We also noticed that the relevant rate value k increases with the discharge current. Such a feature confirms a previous observation relevant to the air corona degradation of phenols for example [24]. In the present study, the linear correlation is not strictly settled due to the difficulty of shortening the sampling and measurement times and the resulting uncertainty.

Although we found it essential to perform a nucleophilic substitution under plasma conditions, we preferred to focus on the changes of the target solution after the discharge is switched off. Such phenomena are referred to as temporal post-discharge reactions [25] which have not been described up to now for a corona discharge, as far as we know.

3.4. Influence of the working parameters of the discharge on the post-discharge kinetics.

The influence of the working parameters of the discharge on the nucleophilic substitution reaction in post-discharge conditions was then examined by varying the current intensity, the electrode gap and the treatment time for the considered example. The polarity of the discharge was fixed and kept positive for the whole study because it appeared to be more efficient than a negative discharge. Also, the “parallel layout” of the electrodes was retained for all the experiments.

3.4.1. Influence of the current intensity I on the post-discharge kinetics

The current I (μA) of the discharge is a key parameter for controlling its efficiency. We varied the current between 50 and 100 μA and kept all the other working parameters constant. As already mentioned, the absorbance of the target solution decreased in post-discharge conditions as the post-discharge time t increased.

Moreover, the matching graphs $\ln |A_\infty - A_t| = f(t)$ are linear (Figure 5): a 1st order kinetic step may reasonably account for the observed evolution. This strongly suggests that activated CO^* goes on diffusing in the target solution and substituting to the leaving group *mpz*.

Also, the negative slopes k of the post-discharge plots $\ln |A_\infty - A_t| = f(t)$ depend on the current intensity of the discharge and k increases with I : $k(\text{s}^{-1}) = 2 \times 10^{-8} I(\mu\text{A})^2 + 9 \times 10^{-7} I(\mu\text{A}) + 6 \times 10^{-7}$, $R^2 = 0.9992$ (Figure 6). This feature agrees with the increase with I of the flux of the activated neutral species CO^* formed in the discharge.

At least we must point out that the ligand exchange reaction is governed by the formation of an electrophilic group, that is by the ability of the plasma to break the bond between the ligand *mpz* and the metal centre. The resulting intermediate develops according to a Lewis acid/base mechanism: CO^* reacts by its free electron pair, and the electrophilic moiety $\text{Fe}(\text{CN})_5$ by its unoccupied orbital.

3.4.2. Influence of the exposure time t^* to the plasma (treatment time t^*)

The exposure time to the corona discharge, also called the treatment time t^* , governs the evolution of the nucleophilic substitution observed in post-discharge conditions. This is well verified through experiments performed in fixed conditions [i.e., $I = 50 \mu\text{A}$; $V = 12.50 \text{ kV}$; $Q_{\text{co}} = 6.67 \text{ cm}^3 \text{ s}^{-1}$; $d = 8 \text{ mm}$.], but for various values of t^* in the range ($10 < t^* (\text{min}) < 42$). As mentioned, the absorbance of the plasma treated solution for t^* minutes decreases in post-discharge conditions, which confirms that the ligand exchange reaction goes on. The log plots $\ln |A_\infty - A_t| = f(t)$ relevant to various values of the treatment time t^* account for the post-discharge changes observed in the solution (Figure 7), i.e., when the discharge is switched off. The relevant plots show that the substitution rate increases with the treatment time t^* : $k(\text{s}^{-1}) = 1.6 \times 10^{-7} t^*(\text{s}) + 2.5 \times 10^{-5}$; $R^2 = 0.9128$ (Figure 8). The relevant slope 1.6×10^{-7} differs from the estimated slope reported in

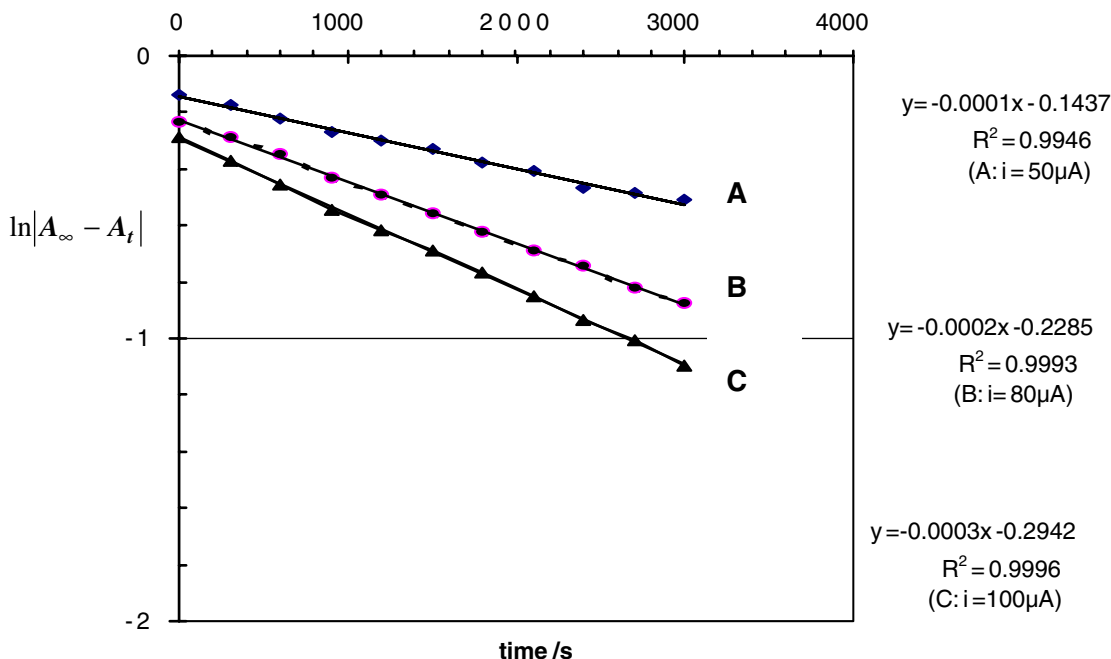


Fig. 5. Effect of the current intensity of the discharge [$I = 50 \mu\text{A}$ (A); $80 \mu\text{A}$ (B); $100 \mu\text{A}$ (C)] on the post-discharge decrease in the absorbance of the treated solution. Working conditions of the plasma treatment: $d_1 = 18 \text{ mm}$; $d_2 = 8 \text{ mm}$; gas flow $= 0.02 \text{ dm}^3 \text{ s}^{-1}$; treatment time $t^* = 600 \text{ s}$.

Figure 4 because the experiments are performed in different conditions of current intensity of the discharge

3.4.3. Influence of the electric charge $I \times t^*$ provided to the discharge

The influence of the electric charge on the post discharge phenomena was sketched out by plotting the variation of $\ln|A_\infty - A_t|$ vs the post-discharge time t , for a given electric charge ($I \times t^* = 36 \text{ mC}$) provided by the discharge. The resulting plots are lines (Figure 9) and the calculated slopes are the more negative the higher the

current intensity of the discharge. This result illustrates how important is the electric charge in the energy transfer from the discharge to the gas as a source of reactive species which are the keys of the considered nucleophilic substitution reaction. However, a linear relationship between k , and the electrical power of the discharge was only very approximately verified (see for example, the various k values illustrated in Figure 9 for a given electric power).

3.4.4. Influence of the electric power P of the discharge on the kinetic constant k

The plot k vs P giving the reaction rate constant k as a function of the electric power P provided to the discharge is very roughly linear, which is expected from other examples of plasmachemical reactions, but the R^2 value is not satisfactory in the present case. This feature may be related to the fact that evaporation phenomena concerning the liquid target take place for long plasma treatments and may modify the mean distance between the liquid surface and the point electrode.

3.5. Choice of the target complex

Changing the starting *fempz* complex by *fepyridine* or *fe4-methylpyridine* allowed us to check the general character of the considered plasmachemical reaction. The new target solutions [4, 5] do not absorb in the same spectral range as the *mpz* complex, and the pyridine complexes are often less stable than the *mpz* ferrate. This does not preclude similar to the reported study and in particular, the plasma substitution of a ligand L by corona activated CO^* . Post-discharge phenomena also occur and confirm our observations.

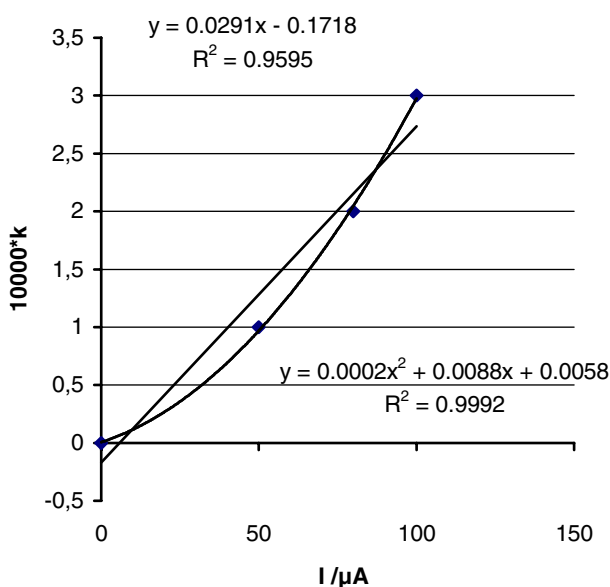


Fig. 6. Influence of the current intensity on the post-discharge kinetic rate: the plot $10^4 k$ fits with the function $10^4 k = 2 \times 10^{-4} I^2 + 88 \times 10^{-4} I + 58 \times 10^{-4}$ ($R^2 = 0.9992$.)

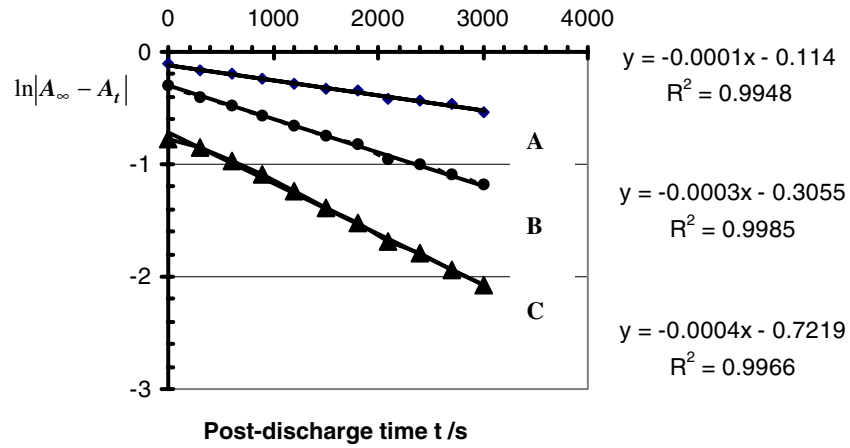


Fig. 7. Effect of the exposure time t^* (s) to the plasma or treatment time on the post-discharge kinetics. Curve A: $t^* = 600$ s; $k = 1.36 \times 10^{-4} \text{ s}^{-1}$. Curve B: $t^* = 1200$ s; $k = 3.05 \times 10^{-4} \text{ s}^{-1}$. Curve C: $t^* = 2520$ s; $k = 4.88 \times 10^{-4} \text{ s}^{-1}$.

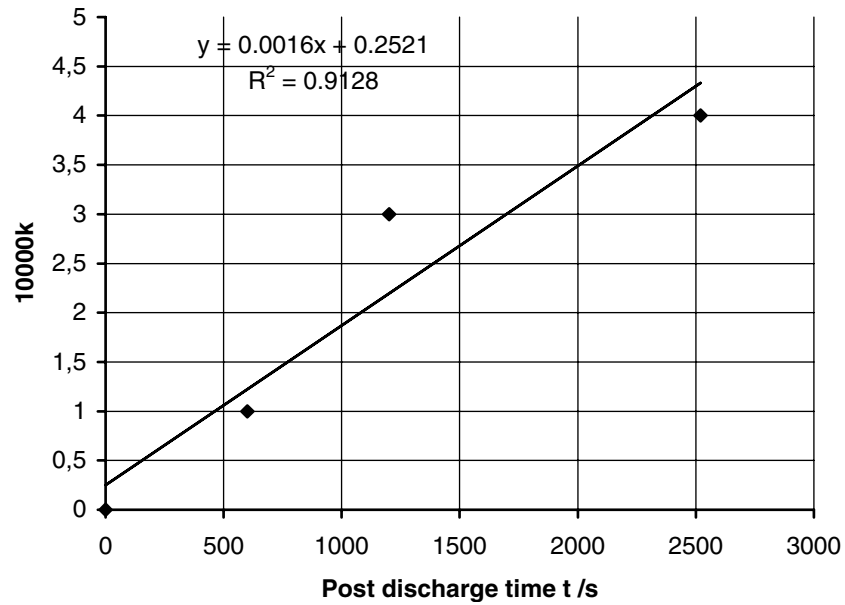


Fig. 8. Variation of the post-discharge kinetic constant $10^4 k (\text{s}^{-1})$ with the post-discharge time t (s) for a fixed electric charge $I \times t^*$.

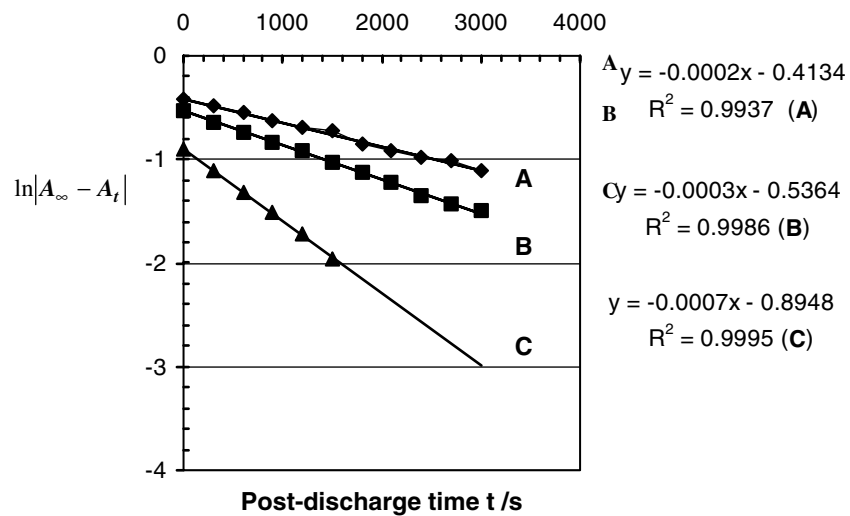
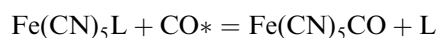


Fig. 9. Post-discharge reactions performed with a constant electric charge ($Q = I \times t^* = 36 \text{ mC}$) provided to the target solution. Curve A: $I = 30 \text{ }\mu\text{A}$; $t^* = 1200$ s; $k = 2 \times 10^{-4} \text{ s}^{-1}$. Curve B: $I = 60 \text{ }\mu\text{A}$; $t^* = 600$ s; $k = 3 \times 10^{-4} \text{ s}^{-1}$. Curve C: $I = 120 \text{ }\mu\text{A}$; $t^* = 300$ s; $k = 7 \times 10^{-4} \text{ s}^{-1}$.

3.6. Side applications to analysis

The reported study shows that the ligand exchange reaction



is realised with various ligands (i.e., N-methylpyrazinium or substituted pyridines for the most usual ones) but only under the smooth plasma conditions provided by a corona discharge. The kinetic results relevant to the exchange reaction may provide us with a convenient technique for measuring the activated CO* at ambient temperature. The applications are numerous, and concern the activated CO* produced in electric discharges or in combustion devices.

One can guess that the method is precise, if the main kinetic factors, such as the target and plasma gas temperatures are carefully controlled. However, the accuracy is probably not be so high since the method is based on kinetic measurements. Further work is necessary to test and improve the method which is at present being developed in the laboratory.

4. Conclusions

This study shows that a particular nucleophilic substitution reaction involving CO requires the smooth conditions of a corona discharge, while it does not occur in the absence of activated species. The kinetics are relatively fast compared with other exchange rates for the same series of complexes, so that the ligand exchange needs a moderate treatment time (30–60 min).

The occurrence of the reported ligand exchange reaction agrees with the Lewis basic character of CO* which is enhanced in the activated state, with respect to CO in the fundamental state.

Other exchange reactions performed on Pyridine (Py) complexes selected in the *fePy* family were successful, and were arguments in favour of the general character of the enhanced reactivity of the activated CO*.

Additionally, we got evidence of post discharge kinetics which took place when the discharge was switched off. The post-discharge exchange reaction was found to be 1st order, which may be related to diffusion phenomena at the plasma liquid boundary or/and in the liquid target. The post-discharge kinetic constants largely depend on the parent reaction performed under plasma conditions. The influence of the major parameters of the discharge (i.e., the current intensity, the treatment time etc) on the post discharge kinetics was investigated.

Such unexpected phenomena are interesting from the following points of view:

First, the reported example deals with a reaction which does not occur under ordinary conditions and accounts for a nucleophilic substitution reaction under plasma conditions.

Second, we report an example of post-discharge reactions in the corona treatment of liquids, which is scientifically of major importance.

Third, the occurrence of post-discharge phenomena presents a major economic interest, because the plasma initiated reaction needs no energy supply to continue.

Additionally, the reaction described is specific to corona activated carbon monoxide; the detailed mechanism and the species involved are still under investigation. It thus represents the principle of an analytical method for measuring activated CO, still under development in the laboratory.

Acknowledgement

This work was supported by the Francophonie AUF 6301-PS-327 co-operation programme.

References

1. F. Basolo, *Pure Appl. Chem.* **60** (1988) 1193.
2. F. Basolo and R.G. Pearson, *Mechanism in Inorganic Reactions*, 2nd ed., (Wiley Eastern Private, New Delhi, 1967), pp. 701.
3. H.E. Toma and L.A. Oliveira, *Org. Chim. Acta.* **33** (1979) 143.
4. J.-L. Brisset and R. Gaboriaud, *Bull. Soc. Chim. Fr.* (1976) 1715.
5. J.-L. Brisset and V. Ilmbi, *Can. J. Chem.* **58** (1980) 1250.
6. D.J. Kenney, T.P. Flynn and J.B. Gallini, *J. Inorg Nucl. Chem.* **20** (1961) 75.
7. E. Toma, N.M. Moroi and M.Y.M. Iha, *An. Acad. Brasil. Cienc.* **54** (1982) 323.
8. H.E. Toma, N.M. Moroi and N.Y.M. Iha, *An. Acad. Brasil. Cienc.* **54** (1982) 315.
9. A. Vogler and H. Kunkely, *Z. Naturforsch.* **30** (1975) 355.
10. H.E. Toma and M. Malin, *Inorg. Chem.* **12** (1973) 1039.
11. K.F. Purcell and J.C. Kotz, *Inorganic Chemistry* (W.B. Saunders, Philadelphia, 1977).
12. K. Harada, S. Nomoto, M. Takasaki, E. Kubota and T. Wada, *Proc. Int. Symp. Plasma Chem.-8*. Tokyo, Jpn, (1987) 754.
13. O. Matsumoto, K. Hoshino and K. Yoshina, *Proc. Int. Symp. Plasma Chem.-8*. Tokyo, Jpn (1987) 851.
14. M. Tezuka and T. Yajima, *Proc. Int. Symp. Plasma Chem.-10*, Bochum, Ge (1991) paper 3: 2–21.
15. M. Tezuka and M. Iwasaki, *Plasma & Ions* **1** (1999) 23.
16. S.K. Sengupta, A.K. Srivastava and R. Singh, *J. Electroanal. Chem.* **427** (1997) 23.
17. A.L. Yerokhin, X. Nie, A. Leyland, A. Maetthews and S.J. Dowe, *Surf. surface coat* **122** (1999) 73.
18. P. Sunka, V. Babicky, M. Clupek, P. Lukes, M. Silmek, J. Schmidt and M. Cernak, *Plasma Sour. Sci. Technol.* **8** (1999) 258.
19. B. Sun, M. Sato and J.S. Clements, *J. Phys. D – Appl. Phys.* **32** (1999) 1908.
20. E.M. Van Veldhuizen and W.R. Rutgers, *Proc. Int. Symp. Plasma Chem-12* (Minneapolis, USA, 1995), pp. 1083.
21. A.K. Sharma, B.R. Locke, P. Arce and W.C. Finney, *Hazard. Waste Hazard. Mat.* **10** (1993) 209.
22. A. Doubla, J.-L. Brisset and J. Amouroux, *Bull. Soc. Chim. Fr.* (1990) 157.
23. J.L. Brisset, J. Lelièvre, A. Doubla and J. Amouroux, *Analisis* **18** (1990) 185.
24. J.-L. Brisset, *J. Appl. Electrochem.* **27** (1997) 179.
25. A. Doubla, F. Abdelmalek, K. Khalifa, A. Addou and J.-L. Brisset, *J. Appl. Electrochem.* **33** (2003) 73.